

1 ***Fifty-six years of Surface Solar Radiation and Sunshine***
2 ***Duration over São Paulo, Brazil: 1961 - 2016***

3

4 ***Marcia Akemi Yamasoe^{1,3}, Nilton Manuel Évora do Rosário²,***
5 ***Samantha Novaes Santos Martins Almeida³, Martin Wild⁴***

6 [1] Departamento de Ciências Atmosféricas, Instituto de Astronomia, Geofísica e
7 Ciências Atmosféricas, Universidade de São Paulo, São Paulo, Brazil

8 [2] Departamento de Ciências Ambientais, Universidade Federal de São Paulo,
9 Diadema, São Paulo, Brazil

10 [3] Seção de Serviços Meteorológicos do Instituto de Astronomia, Geofísica e Ciências
11 Atmosféricas, Universidade de São Paulo, São Paulo, Brazil

12 [4] Institute for Atmospheric and Climate Science, ETH Zurich, Switzerland

13

14 Correspondence to: M. A. Yamasoe (marcia.yamasoe@iag.usp.br)

15

Abstract

16

17 Fifty-six years (1961 – 2016) of daily surface downward solar irradiation,
18 sunshine duration, diurnal temperature range and the fraction of the sky covered by
19 clouds in the city of São Paulo, Brazil, were analysed. The main purpose was to
20 contribute to the characterization and understanding of the dimming and brightening
21 effects on solar global radiation in this part of South America. As observed in most of
22 the previous studies worldwide, in this study, during the period between 1961 and early
23 1980's, a negative trend in surface solar irradiation of was detected in São Paulo,
24 characterizing the occurrence of a dimming effect. Sunshine duration and the diurnal
25 temperature range also presented negative trends, in opposition to the positive trend
26 observed in the cloud cover fraction. However, a brightening effect, as observed in
27 western industrialized countries in more recent years, was not observed. Instead, for
28 surface downward irradiation, the negative trend persisted, with a trend of -0.13 MJm^{-2}
29 per decade, with a p-value of 0.006, for the 56 years of data and in consonance to the
30 cloud cover fraction increasing trend, but not statistically significant, of 0.3 % per
31 decade (p-value = 0.198). The trends for sunshine duration and the diurnal temperature
32 range, by contrast, changed signal, as confirmed by a piecewise linear regression model.
33 Some possible causes for the discrepancy are discussed, such as the frequency of fog
34 occurrence, urban heat island effects, horizontal visibility (as a proxy for aerosol
35 loading variability) and greenhouse gas concentration increase. Future studies on the
36 aerosol effect are planned, particularly with higher temporal resolution as well as
37 modelling studies, to better analyse the contribution of each possible cause.

38

39 **1 Introduction**

40 Ultimately, the downward solar radiation at the surface is the main source of
41 energy that drives Earth’s biological, chemical, and physical processes (Wild et al.,
42 2013, Kren et al., 2017), from local to global scales. Therefore, the assessment of the
43 variability of the downward solar radiation at the surface is a key step in the efforts to
44 understand Earth’s climate system variability. Before reaching the surface, solar
45 radiation can be attenuated mainly by aerosols and clouds, through scattering and
46 absorption processes, and to a lesser extent, through Rayleigh scattering by atmospheric
47 gases, absorption by ozone and water vapor, for example. In this context, during the last
48 half-century, long term changes in the amount of surface solar radiation have been
49 investigated worldwide (Dutton et al., 1991, Stanhill and Cohen 2001, Wild et al. 2005,
50 Shi et al., 2008, Wild, 2009, 2012, Ohvri, et al., 2009). At least two trends have been
51 well established and documented over wide regions of the world, a decline in surface
52 solar radiation between 1950s and 1980s, named “Global Dimming” and an increase,
53 from 1980s to 2000s, termed “Brightening” (Stanhill and Cohen, 2001; Wild, 2009,
54 2012).

55 The global dimming definition, according to Stanhill and Cohen (2001), refers to
56 a widespread and significant reduction in global irradiance, that is the flux of solar
57 radiation reaching the earth’s surface comprising the direct solar beam and the diffuse
58 radiation scattered by the sky and clouds. However, among these studies, while the
59 dimming phase has been a consensus for all locations analysed, the brightening phase
60 was not (Zerefos et al., 2009, Wild, 2012). Over India, for example, the dimming phase
61 seems to last throughout the 2000s (Kumari and Goswami, 2010). The continuous
62 dimming in India and the renewed dimming in China from 2000s, opposing to a
63 persistent brightening over Europe and the United States, have been linked to trends in

64 atmospheric anthropogenic aerosol loadings (Wild, 2012). By contrast, other studies
65 suggested that changes in cloud cover rather than anthropogenic aerosol emissions
66 played a major role in determining solar dimming and brightening during the last half
67 century (Stanhill et al., 2014). Therefore, the drivers of dimming and brightening are a
68 matter of ongoing research and debate (Manara et al., 2016, Kazadzis et al., 2018,
69 Manara et al., 2019, Yang et al. 2019). The role of these trends in the masking of
70 temperature increases due to increasing greenhouse gases (GHG) concentration has
71 been discussed (Wild et al., 2007). Furthermore, a comprehensive assessment of the
72 spatial scale of both dimming and brightening is critical for a conclusive analysis of the
73 likely drivers and implications for the current global climate variability. Large portions
74 of the globe are still lacking any evaluation on this matter, such as Africa (Wild, 2009),
75 which is a challenge for the spatial characterization of both dimming and brightening
76 trends.

77 Among the rare studies focusing on the South American subcontinent, Raichijk
78 (2012) discussed the trends over South America, analysing sunshine duration (SD) data
79 from 1961 to 2004. The author divided South America in five climatic regions. In three
80 of them, also the one where the city of São Paulo is located, statistically significant
81 negative trends were observed on an annual basis, from 1961 up to 1990. From 1991 to
82 2004 a positive trend was observed in four of the five regions with a significance level
83 higher than 90%.

84 The alternative use of SD is mainly due to the lack of a consistent long-term
85 network for the monitoring of surface solar radiation across the continent, therefore
86 alternative proxies have to be found in order to provide an estimate of surface solar
87 radiation long term trends. Another variable commonly used to investigate surface solar
88 radiation trends is the diurnal temperature range (DTR), the difference between daily

89 maximum (T_{\max}) and minimum (T_{\min}) air temperature measured near the surface
90 (Bristow and Campbell, 1984, Wild et al. 2007, Makowski et al. 2008).

91 The present study takes advantage of fifty-six years of a unique high quality
92 concurrent records of surface solar irradiation (SSR), sunshine duration (SD), diurnal
93 temperature range (DTR) and cloud cover fraction (CCF), i.e., the fraction of the sky
94 covered by clouds, from 1961 to 2016, in the city of São Paulo, Brazil, to provide a
95 perspective on dimming and brightening trends with an extended database.

96 Two questions are addressed in this study: 1) How was the decadal variability of
97 SSR over the 56 years of data?; 2) Can SD and DTR be adopted as proxies to infer SSR
98 variability in São Paulo? To answer to these questions, we organize the manuscript as
99 follows: in section 2 we present the data and methods of analysis; section 3 is divided in
100 3 parts. In the first part of that section, we discuss the annual trends in SSR, SD and
101 DTR; in the second, we focus the analysis on horizontal visibility and the number of
102 foggy days; and, in the third part of section 3, we discuss the trends in the maximum
103 and minimum air temperatures near the surface. Section 4 summarizes the main
104 conclusions and discusses possible future work on the subject.

105

106 **2 Observational Data and Methods**

107 The long-term measurements used in this study were collected at the
108 meteorological station operated by the Instituto de Astronomia, Geofísica e Ciências
109 Atmosféricas from the Universidade de São Paulo (IAG/USP), located at latitude
110 23.65° S and longitude 46.62° W, 799 m above sea level. Figure 1 shows the
111 geographical location of the meteorological station. The site is surrounded by a
112 vegetated area due to its location inside a park.

113



114

115 Figure 1 – São Paulo state and a zooming in view of São Paulo Metropolitan Area and
116 the location of the meteorological station of Instituto de Astronomia, Geofísica e
117 Ciências Atmosféricas from Universidade de São Paulo (EM-IAG). Adapted from ©
118 Google Earth (US Dept. of State Geographer – Data SIO, NOAA, U. S. Navy, NGA,
119 GEBCO - Image Landsat/Copernicus).

120

121 The downward solar irradiation has been measured since 1961 using an
122 Actinograph Robitzsch-Fuess model 58d, with 5% instrumental uncertainty (Plana-
123 Fattori and Ceballos, 1988). The long-term variation of the sensor calibration of
124 -1.5 % per decade was taken into account. This trend was estimated by comparing one
125 year of data collected in parallel and at the same site with a brand new Actinograph
126 Robitzsch-Fuess model 58dc, in 2014 and agrees with previous estimations performed
127 by Plana-Fattori and Ceballos (1988) (See supplementary information for details of the
128 comparison). Sunshine duration data was collected with a Campbell-Stokes sunshine
129 recorder (Horseman et al., 2008) from 1933 to the present, while daily maximum and
130 minimum air temperatures were monitored since 1935. Daily maximum and minimum
131 temperatures were used to estimate the diurnal temperature range as it is simply the
132 difference between the maximum and minimum daily temperatures. Diurnal cloud cover
133 fraction was determined from visual inspection made every hour from 7:00 AM to
134 6:00 PM (local time) (Yamasoe et al. 2017).

135 Annual mean values of downward solar irradiation data at the surface were used
136 to characterize dimming and brightening trends while sunshine duration and diurnal
137 temperature range measurements at the same site were used to provide independent
138 information.

139 In order to estimate trends, avoiding autocorrelation in the data, the modified
140 Mann-Kendall trend test proposed by Hamed and Rao (1998) was applied to the
141 variables, while the regression coefficient was estimated based on Sen (1968). A
142 statistically significant trend at the 95% confidence level was detected if the absolute
143 value of Z was above 1.96. We also applied a piecewise linear regression model,
144 proposed by Muggeo (2003) to detect any trend changes.

145 According to the meteorological station records, completely cloud free days are
146 extremely rare in São Paulo, being more common from June to the beginning of
147 September, corresponding to the southern hemisphere wintertime, when dry conditions
148 prevail in the region (Yamasoe et al., 2017). The number of days without clouds per
149 year, from sunrise to sunset, varied from 1 to 23. This extremely low number of clear
150 sky days restricted the analysis in such conditions, mainly at aiming to evaluate the
151 exclusive role of aerosol variability in the long-term trends.

152 To complement the analysis and help interpreting the findings, we included data
153 about the occurrence of fog and horizontal visibility. The first information was analysed
154 in terms of the number of foggy days (NFD). If fog was observed on a given day, the
155 day received the number 1, otherwise, the number is 0. Horizontal visibility, or simply
156 visibility, is recorded every hour, from 7:00 A.M. till midnight, at the meteorological
157 station. Visibility can be affected by haze and fog conditions but is less sensitive to
158 cloud variability. Thus, all-sky visibility data was used as a proxy for aerosol loading
159 (Zhang et al., 2020). However, to avoid the effect of fog on the horizontal visibility, we

160 limited the data from 10:00 AM to 03:00 PM, as, at the location, fog is usually observed
161 either early in the morning or late in the afternoon, when low temperature and high
162 humidity scenarios are more likely to occur in São Paulo. Therefore, the reduction in
163 visibility from 10:00 AM to 03:00 PM is expected to be related to the atmospheric
164 turbidity. The impact of aerosol on SSR is higher from August to October, when
165 advection of smoke plumes from long range transports can reach São Paulo, summing
166 up to the typical increase in the local pollution associated with the dominance of low
167 dispersion scenarios during this time of the year (Yamasoe et al., 2017). This is also
168 when low temperatures and stable atmospheric conditions favour fog formation. Thus,
169 the analysis of both variables is limited to the months of July to October.

170 To verify if the effect of visibility on SSR and SD could be detected, data
171 measured on clear sky days were analysed normalizing SSR by the expected irradiation
172 at the top of the atmosphere (TSR), determining the solar transmittance and minimizing
173 the seasonal variability. Sunshine duration (SD or n) was normalized to the day-length
174 (N). Top of the atmosphere irradiation and the day-length were estimated using
175 formulas proposed by Paltridge and Platt (1976), which also include the variation of
176 Sun-Earth distance.

177

178 **3 Results**

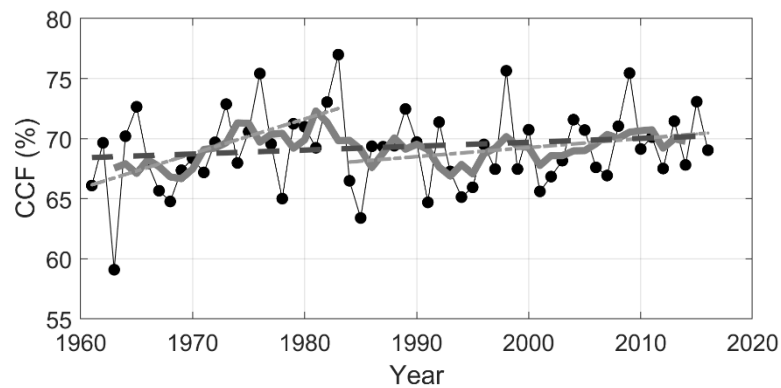
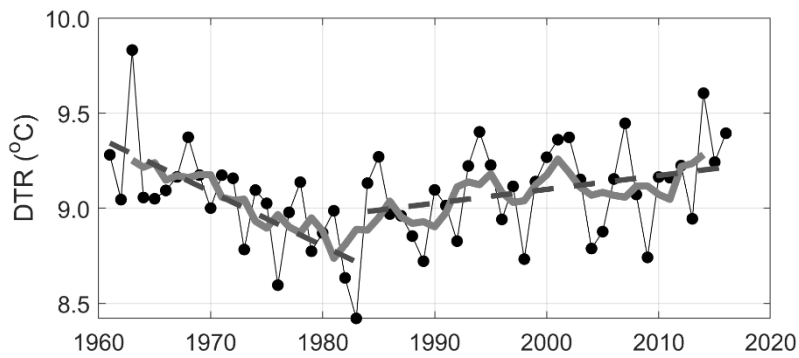
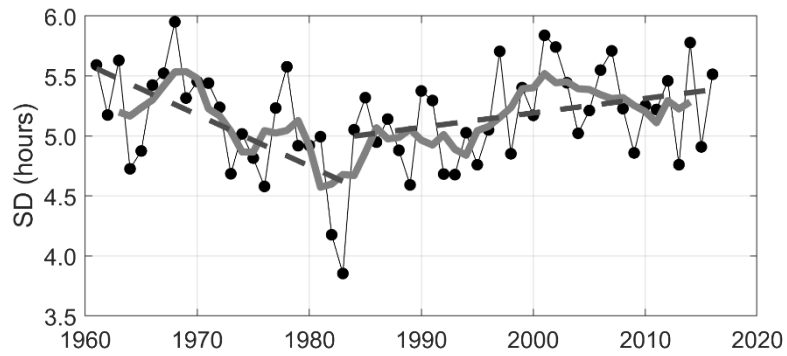
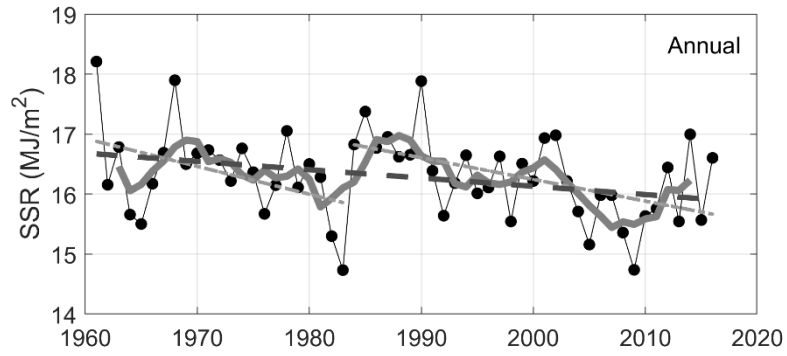
179 **3.1 SSR, SD, DTR and CCF annual mean variability and trends**

180 Figure 2 illustrates the time series of the annual mean values for SSR, SD, DTR
181 and CCF, showing that all the analysed variables exhibited a large variability from year
182 to year. SSR, SD and DTR presented a decreasing trend up to the beginning of the
183 1980's, in opposition, therefore consistent, to the CCF trend. According to Rosas et al.

184 (2019), who analysed the same cloud fraction database from the meteorological station,
185 focusing on the climatology for different cloud types and base heights, all cloud types,
186 except for the middle level clouds, presented a positive trend, which is confirmed by
187 this study.

188

189



190

191

192 Figure 2 – Annual mean variability of surface solar irradiation (SSR), sunshine duration
 193 (SD), diurnal temperature range (DTR) and cloud cover fraction (CCF). Gray curves
 194 represent 5 years moving averages and dotted lines are the result of a trend analysis

195 from 1961 to 1983 and from 1984 to 2016. Lines of the trend analysis for SSR and CCF
196 considering all the analysed years, from 1961 to 2016 are also shown.

197

198 Returning to Fig. 2, the gray curve represents the 5 years moving average, while
199 the dotted lines indicate the result of the modified Mann-Kendall trend analysis,
200 discussed ahead. The year of 1983 was the one presenting the lowest annual mean value
201 for SSR, SD and DTR, clearly as a response to the peak of CCF observed in that year,
202 which is worth to mention, was characterized by a strong El Niño event. According to
203 the Earth System Research Laboratory from the National Oceanic and Atmospheric
204 Administration (ESRL/NOAA), it is listed at the top amongst the 24 strongest El Niño
205 events, in the period from 1895 to 2015, and lasted from April 1982 up to September
206 1983 (<https://www.esrl.noaa.gov/psd/enso/climaterisks/years/top24enso.html>). This
207 1983 El Niño effect was also detected in rainfall data over the São Paulo Metropolitan
208 Area (Obregón et al., 2014), although the authors claim that such influence, at least on
209 rainfall variability, is detectable but is multifaceted and depends on the life cycle of
210 each ENSO event. Xavier et al. (1995), trying to identify a possible influence of ENSO
211 on precipitation extremes in the month of May, classified both May 1983 and May 1987
212 as exceptional extremes of precipitation. Their conclusion was that strong El Niño
213 events can affect the spatial organization of rainfall around São Paulo city. A more
214 recent study performed by Coelho et al. (2017), using daily precipitation data from 1934
215 to 2013 from the same meteorological station analysed in this research, concluded that
216 El Niño conditions in July tend to increase precipitation in the following spring, also
217 anticipating the onset of the rainy season. No study was found about the possible effect
218 of ENSO on cloud cover over São Paulo. According to Rosas et al. (2019), middle and
219 high-level clouds presented high positive anomalous cloud amount in 1983.

220 Applying the piecewise liner regression model (Muggeo, 2003) to detect trend
221 changes, for the variables in Fig. 2, only SD and DTR presented statistically significant
222 breakpoints. For SD, the regime shift was detected in 1982 (± 4 years) ($p = 0.008$) and
223 for DTR, in 1979 (± 4 years) ($p = 0.017$). Considering the uncertainties in the estimates,
224 both include the year 1983, consistent with the findings of Reid et al. (2016), who
225 observed a regime shift in land surface temperature in South America in 1984. These
226 findings motivated us to separate the time series analysis in two periods, the first from
227 1961 to 1983 and the second from 1984 up to 2016. The results of the modified Mann-
228 Kendall trend test for each period and for all the analysed years, from 1961 to 2016, are
229 presented in Table 1, considering both annual and seasonal variabilities. Bold values
230 indicate trends that are statistically significant at the 95% confidence level. From the
231 table, in the first period, SSR, SD and DTR presented a decreasing trend, while CCF a
232 positive one. Except for SSR, all trends were statistically significant, with daily SD
233 decreasing at a rate of 0.37 hours per decade and the diurnal temperature range
234 declining at a rate of 0.49 °C per decade. As detected by the piecewise linear regression
235 model, SD and DTR changed from negative to positive trends, from the first to the
236 second period. Looking at the seasonal variability, southern hemisphere autumn
237 (MAM), winter (JJA) and springtime (SON) presented statistically significant
238 decreasing trends for SD and DTR. For CCF, statistically significant positive trends
239 were observed for JJA and SON and only MAM presented statistically significant
240 positive trend for SSR in the first period. Considering the whole analysed period, only
241 SSR presented statistically significant trend in the annual basis of -0.13 MJm^{-2} per
242 decade. In DJF and MAM, the trends were also negative and statistically significant,
243 while no trends were detected in JJA nor SON. For CCF, a statistically significant trend
244 change was observed only in MAM of almost 1% per decade. For the other seasons and

245 in the annual basis, CCF presented no trend (DJF) or positive trend, but not statistically
 246 significant.

247 Table 1 - Modified Mann-Kendall trend test results for period 1, from 1961 to 1983,
 248 period 2, from 1984 to 2016 and for all the analysed years, from 1961 to 2016,
 249 considering each season and on an annual basis for the surface solar radiation (SSR),
 250 sunshine duration (SD), diurnal temperature range (DTR) and sky cover fraction (CCF).
 251 The trend was estimated as the slope of the linear fit between the variable of interest and
 252 year.

SSR									
	1961-1983			1984-2016			1961-2016		
Time interval	Trend^a	Z	p	Trend^a	Z	P	Trend^a	Z	p
Annual	-0.40	-1.64	0.101	-0.39	-3.02	0.003	-0.13	-2.73	0.006
DJF	-0.64	-1.05	0.291	-0.53	-2.56	0.010	-0.26	-2.94	0.003
MAM	-0.76	-2.48	0.013	-0.25	-1.66	0.097	-0.24	-3.14	0.002
JJA	-0.47	-1.93	0.054	-0.17	-1.87	0.061	0.00	-0.16	0.871
SON	-0.24	-0.89	0.373	-0.57	-2.40	0.016	-0.01	-0.74	0.458

SD									
	1961-1983			1984-2016			1961-2016		
Time interval	Trend^b	Z	p	Trend^b	Z	P	Trend^b	Z	p
Annual	-0.37	-3.41	0.001	0.11	2.13	0.033	0.03	0.56	0.577
DJF	-0.41	-1.06	0.291	-0.01	-0.12	0.905	0.02	0.28	0.783
MAM	-0.53	-2.27	0.023	0.22	1.61	0.107	-0.02	-0.19	0.850
JJA	-0.54	-3.38	0.001	0.20	2.06	0.039	0.05	1.17	0.241
SON	-0.47	-2.31	0.021	0.03	0.20	0.840	0.02	0.33	0.745

DTR									
	1961-1983			1984-2016			1961-2016		
Time interval	Trend^c	Z	p	Trend^c	Z	P	Trend^c	Z	p
Annual	-0.49	-3.33	0.001	0.16	1.84	0.065	0.04	0.80	0.425
DJF	-0.32	-1.61	0.107	0.15	1.72	0.085	0.11	3.94	<10⁻⁴

MAM	-0.58	-2.54	0.011	0.16	1.53	0.125	-0.02	-0.64	0.520
JJA	-0.61	-2.91	0.004	0.14	1.38	0.171	0.06	0.81	0.416
SON	-0.58	-2.64	0.008	0.02	0.17	0.865	0.01	0.13	0.893
CCF									
1961-1983			1984-2016				1961-2016		
Time interval	Trend^d	Z	p	Trend^d	Z	P	Trend^d	Z	p
Annual	2.9	2.48	0.013	0.8	1.78	0.075	0.3	1.29	0.198
DJF	0.5	0.42	0.673	0.3	0.38	0.700	0.0	-0.05	0.961
MAM	2.9	1.58	0.113	0.6	0.76	0.448	0.9	2.28	0.023
JJA	3.5	2.54	0.011	0.8	0.57	0.566	0.2	-0.31	0.756
SON	3.8	2.12	0.034	1.5	1.22	0.221	0.4	1.35	0.180

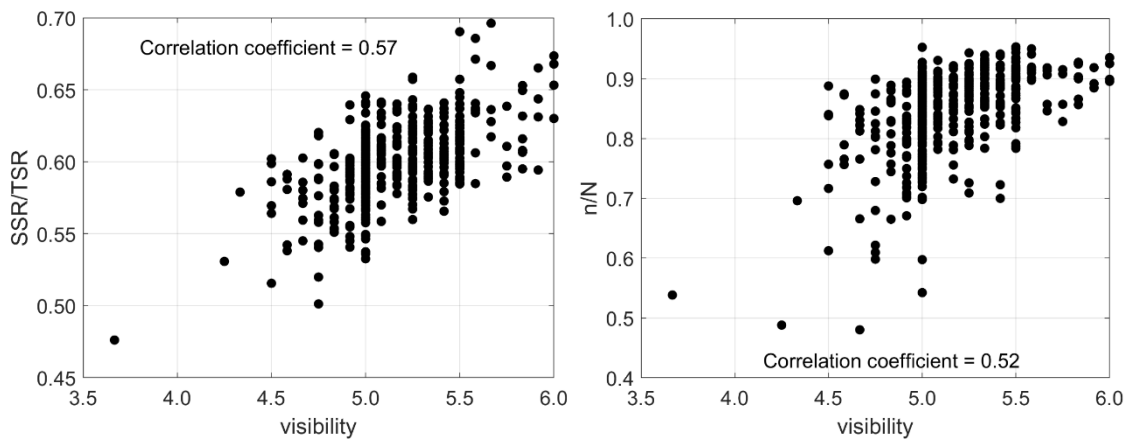
253 Units of trends: a) MJ m⁻² per decade; b) hours per decade; c) °C per decade; d)
254 % per decade

255 In the first period, SSR and its proxies presented trends consistent with CCF
256 features, i.e., as CCF increased over time, the others decreased. In the second period,
257 from 1984 to 2016, this behaviour combination changed. SD and DTR trends changed
258 from negative to positive, being statistically significant only for SD, with a trend of
259 0.11 hours per decade. CCF continued to present a positive trend, but not statistically
260 significant. It is worth noting that, even though the trends are not statistically
261 significant, the pattern between SSR and CCF was observed throughout the entire
262 period. According to Rosas et al. (2019), statistically significant trends, positive for low
263 clouds (3.2 % per decade) and negative for mid-level clouds (-5.5 % per decade), were
264 observed in the last 30 years, from 1987 to 2016. Such analysis indicated that changes
265 in cloud types also influenced the variability of SSR and proxies. However, other
266 factors, rather than only cloud cover changes, were also responsible for the variability of
267 SD and DTR, as evaluated in the next sections.

268 **3.2 Long-term variability of horizontal visibility and of the number of foggy days**

269 To verify how effectively the horizontal visibility acts as a proxy for aerosol
270 optical depth, Fig. 3 shows the solar transmittance (SSR/TSR) and the normalized
271 sunshine duration (n/N) for clear sky days, from July to October, as a function of daily
272 mean visibility. The correlation coefficients are 0.57 and 0.52 for (SSR/TSR) and (n/N),
273 respectively, as indicated in the figure, and for this reason, the visibility data will be
274 analysed next as a proxy for aerosol optical depth. As mentioned in the methodology
275 section, we excluded visibility data from early morning and late afternoon to minimize
276 the influence of fog.

277



278

279 Figure 3 – Daily solar transmittance and the normalized sunshine duration as functions
280 of the mean horizontal visibility recorded from 10:00 AM to 03:00 PM on clear sky
281 days in the months of July to October.

282

283 Figure 4 presents the mean visibility from July to October and registered
284 between 10:00 AM to 03:00 PM, and the number of foggy days in the same months,
285 from 1961 to 2016, both for all sky conditions. July to October are the months with
286 lower cloud cover fraction and with higher probability of long-range transport of

287 biomass burning aerosol particles towards São Paulo, contributing to higher aerosol
288 optical depth in the city (Castanho and Artaxo, 2001, Landulfo et al., 2003, Freitas et
289 al., 2005, Castanho et al., 2008, Yamasoe et al., 2017). Since clear sky days are rare in
290 São Paulo, here we discuss the long-term variability of visibility, trying to infer aerosol
291 loading variations.

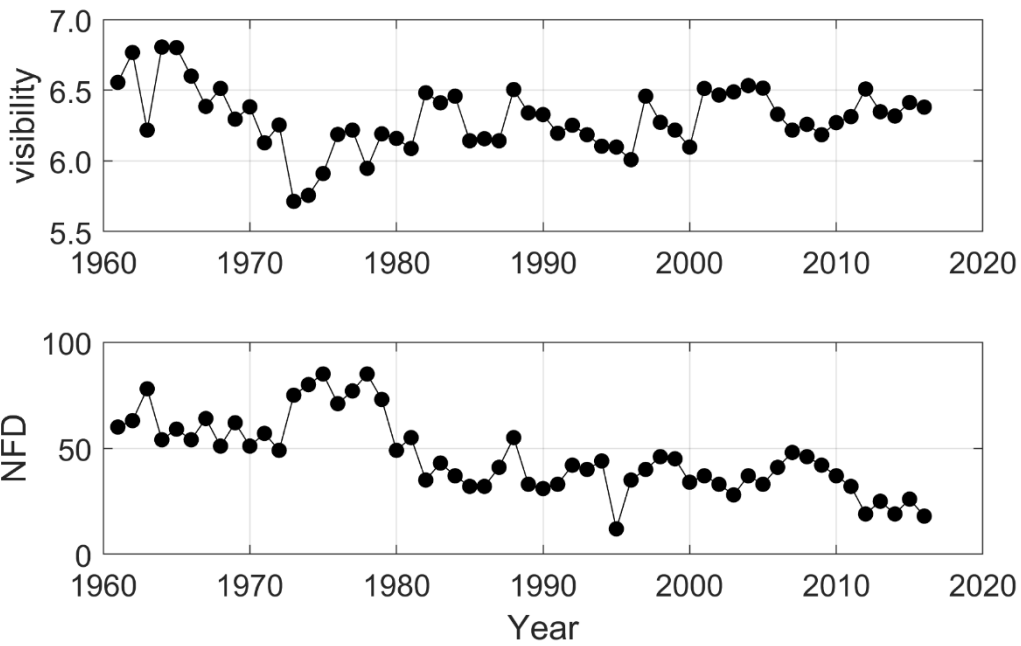
292 From the figure, we see that the highest visibility was observed during the first
293 half of the 1960's, with a gradual degradation till the early 1970's. Thereafter, visibility
294 increased again but never recovered to the values of the 1960's. A significant reduction
295 in visibility was observed in 1963. One hypothesis for the lower visibility in 1963 worth
296 investigating was a sequence of vegetation fires reported in August and September in
297 the state of Paraná affecting 128 municipalities (Paixão and Priori, 2015). Soares (1994)
298 stated that about 10 % of Paraná state was affected by the fires, being responsible for
299 the beginning of fire monitoring in Brazil due to its large proportion. Paraná is located
300 to the south-southwest of the São Paulo state. Cold front systems frequently advect air
301 masses from this region towards São Paulo.

302 Considering local pollution sources, the reduction of the visibility data at the
303 beginning of the series could be associated with the industrialization process in São
304 Paulo, and with the vehicular fleet and changes in the fuel composition, at the end.
305 According to Silva (2011), during 1956 to 1961, a national development plan was
306 implemented in Brazil, to enhance the economic growth, which benefited particularly
307 the city of São Paulo, attracting industries, mainly from the automobile sector. This
308 contributed to increasing the city's population and to the concentration of industries,
309 boosting the economy of São Paulo city. In the 1970's, the high rate of urbanization,
310 with many traffic jams, caused air quality and environmental degradations (Silva,
311 2011). As one of the consequences, the federal government promoted incentives to

312 move industries to other Brazilian states, especially in the north and northeast regions of
313 the country, but a part remained in the Metropolitan Area of São Paulo. Still according
314 to the author, this industrial decentralization process lasted till around 1991.

315 Andrade et al. (2017), discussing changes over time in air quality conditions in
316 the Metropolitan Area of São Paulo, showed that SO₂ frequently exceeded the air
317 quality standards in the 1970's and 1980's. According to the authors, the Brazilian
318 government started a program to control its emissions due to the complaints of the
319 population. At the beginning, the program focused on stationary sources (industries)
320 and, in the 1990's, the sulfur content in diesel fuel was also targeted. Nonetheless,
321 during that decade, the Metropolitan Area of São Paulo still experienced severe air
322 pollution problems with increasing concentration of aerosol particles, which might
323 explain the reduction in visibility at the beginning of the decade (Fig. 4). Over time,
324 SO₂ emission control and other measures helped decreasing the concentration of SO₂
325 and of particulate matter with diameter less than 10 µm (PM₁₀) near the surface.
326 However, according to Oyama (2015), also due to a political decision to stimulate the
327 economy, the annual number of registrations of new gasoline fuelled vehicles increased
328 exponentially, from about 3000 vehicles in 1988, peaking in 2000 with 150000
329 registrations, and decreasing slowly after that, to about 60000 in 2012. Despite the
330 efforts to reduce vehicular emission, the concentration of particulate matter with
331 diameter less or equal 2.5 µm is not yet controlled. In the recent years, vehicular
332 emission is the main local source of air pollution in the Metropolitan Area of São Paulo
333 (Andrade et al., 2017).

334



335

336 Figure 4 – Time series of the mean visibility recorded from 10:00 AM to 03:00 PM and
 337 the number of foggy days (NFD) per year in all sky conditions. Data are limited to the
 338 months of July to October.

339

340 Since both SSR and SD presented positive correlation with visibility, another
 341 factor might be responsible for the opposite trends observed in the second period for
 342 those variables. Changes in the number of foggy days are explored to verify if its
 343 variability can help to explain part of the variability observed in the SD trends,
 344 particularly after 1983, when CCF only could not explain it. As shown in Fig. 4, the
 345 number of days with fog, in the months of July to October each year, is decreasing in
 346 São Paulo. The highest numbers were observed during the 1970's with a sharp decrease
 347 in the end of the decade and the beginning of the next, followed by a long period of
 348 stable conditions up to 2011 when another decrease was observed. This could be the
 349 reason for the positive trend of SD under all sky scenarios in the second period (Fig. 2),
 350 when the CCF increase was not significant. A decrease in the annual number of foggy

351 days was also observed in China (Li et al., 2012), which the authors attributed to the
352 urban heat island effect. São Paulo, throughout the analysed period in this study,
353 experienced a significant change in its spatial domain, which contributed to the
354 intensification of the urban heat island effect. More on this effect will be discussed in
355 the next section.

356

357 **3.3 Long term trends in daily maximum and minimum temperatures**

358 Figure 5 presents the temporal variation of the annual mean of the daily
359 maximum and minimum temperatures registered at the meteorological station, used to
360 estimate DTR. As discussed in the last section, if the increasing trend in SD over the
361 last years could be possibly attributed to the decreasing number of days per year with
362 fog occurrence, we now hypothesize on the possible reasons for the increasing trend of
363 DTR in the second period. According to Dai et al. (1999), DTR should also respond to
364 cloud cover and precipitation and thus to SSR variations. As discussed by the authors,
365 clouds can reduce T_{\max} and increase T_{\min} , since they can reflect solar radiation back to
366 space during daytime and emit thermal radiation down to the surface during the night,
367 respectively. Such behaviours can be clearly seen in Fig. 5, in the first period, and
368 confirmed by the trend analysis presented in Table 2. During the dimming period, T_{\max}
369 presented a negative trend, while T_{\min} an increasing one, statistically significant at 95 %
370 confidence level for the latter variable. A similar behaviour was observed by Wild et al.
371 (2007) who argued that the decreasing trend of T_{\max} is consistent with the negative trend
372 of SSR, demonstrating that solar radiation deficit at the surface presented a clear effect
373 on the surface temperature. Looking at the second period, from 1984 to 2016, both
374 maximum and minimum temperatures presented increasing trend, statistically
375 significant at the 95 % confidence level, on an annual basis, of 0.25 °C per decade and

376 0.16 °C per decade, respectively. In this period, the T_{\min} trend was still in line with the
 377 increasing CCF trend, but as pointed out by Wild et al. (2007) it could also be a
 378 response to the increasing levels of greenhouse gases as also pointed out by de Abreu et
 379 al. (2019) for the south-eastern part of Brazil where São Paulo is located. Like SSR and
 380 CCF, these variables presented no statistically significant regime shift when applying
 381 the piecewise regression model. Thus, considering the whole period, it is possible to
 382 observe that regardless of the season or in the annual basis, both T_{\max} and T_{\min} presented
 383 statistically significant positive trends. T_{\max} increased with a trend of about 0.30 °C per
 384 decade and T_{\min} at a rate of 0.25 °C per decade, being the highest trend detected in the
 385 summer months of DJF.

386

387 Table 2 - Modified Mann-Kendall trend test results for period 1, from 1961 to 1983,
 388 period 2, from 1984 to 2016, and all the analysed years, from 1961 to 2016, considering
 389 each season and in an annual basis, for the daily maximum (T_{\max}) and minimum (T_{\min})
 390 temperatures. The trend was estimated as the slope of the linear fit between the variable
 391 of interest and year.

392

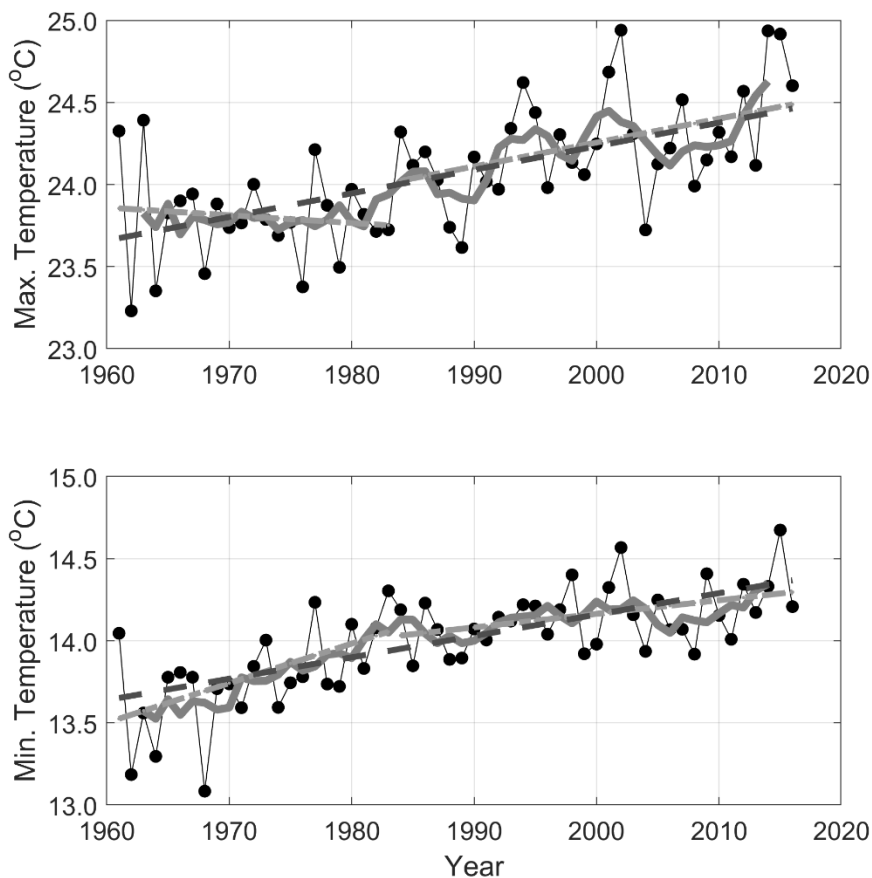
Tmax									
	1961-1983			1984-2016			1961-2016		
Time interval	Trend	Z	p	Trend	Z	p	Trend	Z	p
Annual	-0.11	-1.33	0.184	0.25	2.15	0.031	0.30	4.69	<10⁻⁵
DJF	0.20	1.06	0.291	0.33	2.07	0.038	0.42	4.91	<10⁻⁶
MAM	-0.15	-0.79	0.430	0.03	0.23	0.816	0.22	3.25	0.001
JJA	0.02	0.26	0.795	0.33	2.68	0.007	0.23	3.17	0.023
SON	-0.26	-0.63	0.526	0.36	1.72	0.085	0.32	3.23	0.001

Tmin									
	1961-1983			1984-2016			1961-2016		
Time interval	Trend	Z	p	Trend	Z	p	Trend	Z	p

interval									
Annual	0.56	2.54	0.011	0.16	2.15	0.031	0.25	5.68	<10⁻⁷
DJF	0.53	2.96	0.003	0.13	2.68	0.007	0.31	5.66	<10⁻⁷
MAM	0.52	2.71	0.007	-0.07	-0.79	0.429	0.27	3.17	0.002
JJA	0.62	1.58	0.113	0.26	1.78	0.075	0.18	2.66	0.008
SON	-0.03	0.63	0.526	0.26	2.43	0.015	0.27	6.68	<10⁻⁹

393 Units of trend: °C per decade

394



395

396 Figure 5 - Annual mean variability of daily maximum and minimum air temperatures at
 397 1.5 meters. Gray curves represent 5 years moving averages, light-gray-dotted lines are
 398 the result of trend analysis from 1961 to 1983 and from 1984 to 2016 and the dark-gray-
 399 dotted line represents the trend from 1961 to 2016.

400

401 The urban heat island (UHI) effect could also be responsible for the observed
 402 increasing trend of T_{max} , particularly after 1980. The Metropolitan Area of São Paulo
 403 experienced a fast growth rate from 1980 to 2010. There were nearly 12 million

404 inhabitants in 1980, and the population grew to about 21 million inhabitants in 2010
405 (Silva et al., 2017). According to the authors, the urban area increased from 874 km² to
406 2209 km², from 1962 to 2002. According to Kim and Baik (2002), the maximum UHI
407 intensity is more pronounced in clear sky conditions, occurs more frequently at night
408 than during the day, and decreases with increasing wind speed. However, Ferreira et al.
409 (2012) reported that, in São Paulo, the urban heat island maximum effect was observed
410 during daytime, around 03:00 PM, and was associated with downward solar radiation
411 heating the urban region in a more effective way than the rural surrounding areas.

412 Finally, as pointed out by Wild et al. (2007), the increasing atmospheric
413 concentration of greenhouse gases (GHG) can be another reason for the observed trend
414 of T_{\max} , which was masked by the dimming effect in the first period. Modelling studies
415 can help verify the real causes and disentangle the contribution of each effect, which is,
416 however, out of the scope of this work.

417

418 **4 Conclusions**

419 This analysis of 56 years of surface solar irradiation (SSR) and proxies (SD and
420 DTR) data helped to show that from about 1960 to the early 1980s, named as first
421 period, a dimming effect of surface solar radiation was observed in the city of São
422 Paulo, consistent with other parts of the world. The positive trend of CCF in the first
423 period indicates that cloud cover changes could be one important driver of the dimming
424 period. The dimming effect was also confirmed by SD and DTR trends in the mentioned
425 period. However, the consistency between SSR, SD and DTR trends ended around
426 1983, when CCF presented the highest value throughout the entire series and which
427 coincided with a strong El Niño year. Thus, answering our first question, SSR presented
428 a decreasing trend, throughout the 56 years of data, statistically significant at the 95%

429 confidence level, with a rate of -0.13 MJ m^{-2} per decade. The negative trend was
430 statistically significant also in DJF and MAM, presenting the most negative trend in the
431 summer (DJF) of -0.26 MJ m^{-2} per decade.

432 Applying a piecewise linear regression model to the variables, only SD and DTR
433 presented a statistically significant regime shift, around 1982 and 1979, respectively,
434 with uncertainty of four years in both results. As the negative SSR trend was consistent
435 with the slight positive trend of CCF, the changing behaviour of SD and DTR indicated
436 that other factors besides the cloud cover variability might have affected their distinct
437 patterns. In order to understand the possible causes of the SD trends, alternative
438 parameters (fog frequency and horizontal visibility) focusing on the dry months of July
439 to October, were analysed. The results indicated that the decreasing trend of the number
440 of foggy days per year may explain part of the increasing trend of SD.

441 Moreover, on clear sky days, both SSR and SD presented correlation coefficients
442 above 0.5 with visibility for the period when fog is unlikely to occur, indicating that this
443 variable could be used as a proxy for aerosol loading variations. Changes in visibility
444 during the 1960s and 1970s could be associated with the dynamics of the
445 industrialization process of São Paulo Metropolitan Area and the consequent
446 urbanization, with population growth, traffic jams and the degradation of the air quality.
447 Long-range transport of biomass burning products towards São Paulo is also an
448 important source of aerosol during the dry season. However, the long-term contribution
449 of the different regions, as sources of pollutants to the atmosphere of the Metropolitan
450 Area of São Paulo is unclear. The role of biomass burning, in the state of São Paulo and
451 the neighbour states of Minas Gerais, Paraná and Mato Grosso, is yet to be clarified.
452 Further research is needed to improve our historical perspective on the role of other
453 regional air pollution sources on the SSR.

454 In the case of DTR, since it was obtained from the difference between the daily
455 maximum and minimum air temperatures close to the surface, the trends of the annual
456 mean values of these temperatures were separately determined and analysed. The T_{\min}
457 positive trends followed the CCF ones, with also a possible influence of the increasing
458 levels of greenhouse gases, noticing that the reduction observed in CCF, in the
459 beginning of the second period, is absent in the T_{\min} time series. The increasing trend of
460 CCF, in the first period, resulted in a decreasing trend in T_{\max} , as more solar radiation
461 reaching the surface was attenuated from year to year due to the presence of clouds.
462 Some hypotheses for the increasing trend of T_{\max} during the second period were the
463 urban heat island effect and the increasing concentrations of GHG. Of course, changes
464 in the wind pattern and consequently in the advection of air masses with distinct
465 properties can also affect the air temperature locally.

466 As the resultant trends of SD and DTR, compared with the SSR trend, diverged
467 in the second period for São Paulo, in all sky conditions, caution might be taken when
468 those variables are used as proxies to downward surface solar radiation in the context of
469 dimming and brightening analyses. This study revealed that different factors may act on
470 each variable, leading to a distinct behaviour, as also mentioned by Manara et al.
471 (2017).

472 For future studies, modelling efforts may be able to help evaluate each
473 hypothesis raised in the present study, either those related to climate natural variability,
474 such as El Niño, or those arising from anthropogenic activities as the increase of
475 greenhouse gas concentrations, land use changes, particularly through the
476 imperviousness of soils, affecting the partitioning of latent and sensible heat fluxes.
477 Also, a higher temporal analysis and simultaneous monitoring of aerosol optical

478 properties will help to better evaluate the aerosol effect on downward solar radiation in
479 this region, including via the indirect effect.

480

481 **Data availability**

482 Access to IAG meteorological station database (sky cover fraction, sunshine duration,
483 daily maximum and minimum air temperatures, number of foggy days, visibility and
484 irradiation data) for education or scientific use can be made under request at
485 http://www.estacao.iag.usp.br/sol_dados.php. All processed data used in the manuscript
486 such as annual and seasonal mean values, as well as data from cloud free days can be
487 found at [https://www.iag.usp.br/lraa/index.php/data/cientec/weather-station-
488 climatology/](https://www.iag.usp.br/lraa/index.php/data/cientec/weather-station-climatology/).

489

490 **Author contribution**

491 Conceptualization MAY and NMER; Methodology MAY; Data organization MAY and
492 SNSMA; Formal analysis MAY; Writing original draft MAY and NMER; Writing –
493 Review & Editing MAY, NMER, MW.

494

495 **Competing interest**

496 The authors declare that they have no conflict of interest.

497

498 ***Acknowledgements***

499 The authors acknowledge Fundação de Amparo à Pesquisa do Estado de São Paulo
500 (FAPESP), grant number 2018/16048-6 and Coordenação de Aperfeiçoamento de

501 Pessoal de Nível Superior (CAPES) for financial support. Yamasoe acknowledges
502 CNPq (Conselho Nacional de Desenvolvimento Científico e Tecnológico), process
503 number 313005/2018-4. Global dimming and brightening research at ETH Zurich is
504 funded by the Swiss National Science Foundation (Grant number 200020 188601). This
505 study is part of the Núcleo de Apoio à Pesquisa em Mudanças Climáticas (INCLINE)
506 and of Processos Radiativos na Atmosfera – Impactos dos Gases, Aerossóis e Nuvens.
507 The authors are grateful to the observers and staff of the Instituto de Astronomia,
508 Geofísica e Ciências Atmosféricas meteorological station for making available the
509 meteorological observations. The authors acknowledge the two anonymous referees for
510 their time, comments and suggestions that helped improve and clarify this paper.

511

512

513 **References**

- 514 Andrade, M. F., Kumar, P., Freitas, E. D., Ynoue, R. Y., Martins, J., Martins, L. D.,
515 Nogueira, T., Perez-Martinez, P., Miranda, R. M., Albuquerque, T., Gonçalves, F. L. T.,
516 Oyama, B. and Zhang, Y. Air quality in the megacity of São Paulo: Evolution over the
517 last 30 years and future perspectives. *Atmospheric Environment* 159, 66-82, 2017.
- 518 Bristow, K. L. and Campbell, G. S. On the relationship between incoming solar
519 radiation and daily maximum and minimum temperature. *Agricultural and Forest*
520 *Meteorology* 31, 159-166, 1984.
- 521 Castanho, A. D. A. and Artaxo, P. Wintertime and summertime São Paulo aerosol
522 source apportionment study. *Atmospheric Environment* 35, 4889-4902, 2001.
- 523 Castanho, A. D. de A., Martins, J. V. and Artaxo, P. MODIS aerosol optical depth
524 retrievals with high spatial resolution over an urban area using the critical reflectance. *J.*
525 *Geophys. Res.* 113, D02201, doi: 10.1029/2007JD008751, 2008.
- 526 Coelho, C. A. S., Firpo, M. A. F., Maia, A. H. N., and MacLachlan, C. Exploring the
527 feasibility of empirical, dynamical and combined probabilistic rainy season onset
528 forecasts for São Paulo, Brazil. *Int. J. Climatol.* 37 (Suppl. 1), 398-411, doi:
529 10.1002/joc.5010, 2017.
- 530 Dai, A., Trenberth, K. E. and Karl, T. R. Effects of clouds, soil moisture, precipitation,
531 and water vapor on diurnal temperature range. *Journal of Climate* 12, 2451-2473, 1999.

532 de Abreu, R. C., Tett, S. F. B., Schurer, A. and Rocha, H. R. Attribution of detected
533 temperature trends in Southeast Brazil. *Geophysical Research Letters*, 46, 8407–8414.
534 <https://doi.org/10.1029/2019GL083003>, 2019.

535 Dutton, E. G., Stone, R. S., Nelson, D. W. and Mendonca, B. G. Recent interannual
536 variations in solar radiation, cloudiness, and surface temperature at the South Pole.
537 *Journal of Climate* 4, 848-858, 1991.

538 Ferreira, M. J., Oliveira, A. P., Soares, J., Codato, G., Bárbaro, E. W. and Escobedo, J.
539 F. Radiation balance at the surface in the city of São Paulo, Brazil: diurnal and seasonal
540 variations. *Theor. Appl. Climatol.* 107-229-246. doi: 10.1007/s00704-011-0480-2,
541 2012.

542 Freitas, S. R., K. M. Longo, M. A. F. S. Dias, P. L. S. Dias, R. Chatfield, E. Prins, P.
543 Artaxo, G. A. Grell, and F. S. Recuero. Monitoring the transport of biomass burning
544 emissions in South America, *Environ. Fluid Mech.*, 5, 135–167, 2005.

545 Hamed, K. H. and Rao, A. R. A modified Mann-Kendall trend test for autocorrelated
546 data. *Journal of Hydrology* 204, 182-196, 1998.

547 Horseman, A., MacKenzie, A. R. and Timmis, R. Using bright sunshine at low-
548 elevation angles to compile an historical record of the effect of aerosol on incoming
549 solar radiation. *Atmos. Environ.* 42, 7600-7610, 2008.

550 Kazadzis, S., Founda, D., Psiloglou, B. E., Kambezidis, H., Mihalopoulos, N., Sanchez-
551 Lorenzo, A., Meleti, C., Raptis, P. I., Pierros, F., and Nabat, P. Long-term series and
552 trends in surface solar radiation in Athens, Greece, *Atmos. Chem. Phys.*, 18, 2395–
553 2411, <https://doi.org/10.5194/acp-18-2395-2018>, 2018.

554 Kim, Y.H. and Baik J. J. Maximum urban heat island intensity in Seoul. *J. Appl.*
555 *Meteorol*, 41, 651–659, 2002.

556 Kren, A. C., Pilewskie, P. and Coddington, O. Where does Earth’s atmosphere get its
557 energy? *J. Space Weather Space Clim.* 7(A10) doi: 10.1051/swsc/2017007, 2017.

558 Kumari, B. P. and Goswami, B. N. Seminal role of clouds on solar dimming over India
559 monsoon region. *Geophys. Res. Letters* 37 (L06703), 1-5, doi:10.1029/2009GL042133,
560 2010.

561 Landulfo, E., A. Papayannis, P. Artaxo, A. D. A. Castanho, A. Z. Freitas, R. F. Sousa,
562 N. D. Vieira Jr., M. P. M. P. Jorge, O. R. Sánchez-Ccoyllo, and D. S. Moreira.
563 Synergetic measurements of aerosols over São Paulo, Brazil using LIDAR,
564 Sunphotometer and satellite data during the dry season, *Atmos. Chem. Phys.*, 3, 1523–
565 1539, 2003.

566 Li, Z., Yang, J., Shi, C. and Pu, M. Urbanization effects on fog in China: Field Research
567 and Modeling. *Pure Appl. Geophys.* 169, 927-939, doi: 10.1007/s00024-011-0356-5,
568 2012.

569 Makowski, K., Wild, M. and Ohmura, A. Diurnal temperature range over Europe
570 between 1950 and 2005. *Atmos. Chem. Phys.*, 8, 6483–6498, 2008.

571 Manara, V., Brunetti, M., Celozzi, A., Maugeri, M., Sanchez-Lorenzo, A. and Wild, M.
572 Detection of dimming/brightening in Italy from homogenized all-sky and clear-sky
573 surface solar radiation records and underlying causes (1959-2013). *Atmos. Chem. Phys.*
574 16, 11145-11161, doi:10.5194/acp-16-11145-2016, 2016.

575 Manara, V., Brunetti, M., Maugeri, M., Sanchez-Lorenzo, A. and Wild, M. Sunshine
576 duration and global radiation trends in Italy (1959–2013): To what extent do they agree?
577 *J. Geophys. Res. Atmos.* 122, 4312–4331, doi:10.1002/2016JD026374, 2017.

578 Manara, V., Bassi, M., Brunetti, M. et al. 1990–2016 surface solar radiation variability
579 and trend over the Piedmont region (northwest Italy). *Theor. Appl. Climatol.* 136, 849–
580 862, doi: 10.1007/s00704-018-2521-6, 2019.

581 Muggeo, V. M. R. Estimating regression models with unknown break-points. *Statist.*
582 *Med.* 22, 3055–3071. doi: 10.1002/sim.1545, 2003.

583 Obregón G. O., Marengo J. A. and Nobre C. A. Rainfall and climate variability: long-
584 term trends in the Metropolitan Area of São Paulo in the 20th century. *Clim Res* 61:93-
585 107. <https://doi.org/10.3354/cr01241>, 2014.

586 Ohvriil, H., Teral, R., Neiman, L., Kannel, M., Uustare, M., Tee, M., Russak, V.,
587 Okulov, O., Jõeveer, A., Kallis, A., Ohvriil, T., Terez, E. I., Terez, G. A., Gushchin, G.
588 K., Abakumova, G. M., Gorbarenko, E. V., Tsvetkov, A. V. and Laulainen, N. Global
589 dimming and brightening versus atmospheric column transparency, Europe, 1906-2007.
590 *J. Geophys. Res.* 114(D00D12), 1-17, doi:10.1029/2008JD010644, 2009.

591 Oyama, B. S. Contribution of the vehicular emission to the organic aerosol composition
592 in the city of São Paulo. (Doctoral Thesis). Universidade de São Paulo, São Paulo,
593 Brazil. Available at
594 https://www.iag.usp.br/pos/sites/default/files/t_beatriz_s_oyama_corrigida.pdf - last
595 access on October 25, 2019, 2015.

596 Paixão, L. A. and Priori, A. A. Social and environmental transformations of the rural
597 landscape after an environmental disaster (Paraná, Brazil, 1963). *Estudos Históricos*
598 28(56), 323-342, <http://dx.doi.org/10.1590/S0103-21862015000200006>, 2015.

599 Paltridge, G. W. and Platt, C. M. R. Radiative processes in meteorology and
600 climatology. Elsevier Science, Amsterdam, Oxford, New York, 1976.

601 Plana-Fattori, A. and Ceballos, J. C. Algumas análises do comportamento de um
602 actinógrafo bimetálico Fuess modelo 58d. *Revista Brasileira de Meteorologia* 3 (2),
603 247-256, 1988.

604 Raichijk, C. Observed trends in sunshine duration over South America. *International*
605 *Journal of Climatology* 32, 669-680. doi: 10.1002/joc.2296, 2012.

606 Reid, P. C., Hari, R. E., Beaugrand, G., Livingstone, D. M., Marty, C., Straile, D.,
607 Barichivich, J., Goberville, E., Adrian, R., Aono, Yasuyuki, Brown, R., Foster, J.
608 Groisman, P., Hélaouët, P., Hsu, H.-H., Kirby, R., Knight, J., Kraberg, A., Li, J., Lo, T.-
609 T., Myneni, R. B., North, R. P., Pounds, J. A., Sparks, T., Stübi, R., Tian, Y., Wiltshire,

610 K. H., Xiao, D. and Zhu, Z. Global impacts of the 1980s regime shift. *Global Change*
611 *Biology* 22, 682-703. doi: 10.1111/gcb.13106, 2016.

612 Rosas, J., Yamasoe, M. A., Sena E. T. and Rosário N. E. Cloud climatology from visual
613 observations at São Paulo, Brazil. *Int. J. Climatol.*, 1–13.
614 <https://doi.org/10.1002/joc.6203>, 2019.

615 Sen, P. K. Estimates of the regression coefficient based on Kendall's Tau. *Journal of the*
616 *American Statistical Association* 63(324), 1379-1389, 1968.

617 Shi, G., Hayasaka, T., Ohmura, A., Chen, Z.-H., Wang, B., Zhao, J.-Q., Che, H.-Z. and
618 Xu, Li. Data quality assessment and the long-term trend of ground solar radiation in
619 China. *Journal of Applied Meteorology and Climatology* 47, 1006-1016, 2008.

620 Silva, F. B., Longo, K. M., and Andrade, F. M. Spatial and temporal variability patterns
621 of the urban heat island in São Paulo. *Environments* 4, 27, doi:
622 10.3390/environments4020027, 2017.

623 Silva, P. F. J. Notas sobre a industrialização no estado de São Paulo, Brasil. *Finisterra*,
624 XLVI 91, 87-98, 2011.

625 Soares, R. V. Ocorrência de incêndios em povoamentos florestais. *Floresta* 22(1/2), 39-
626 53, 1994.

627 Stanhill, G. and Cohen, S. Global dimming: a review of the evidence for a widespread
628 and significant reduction in global radiation with discussion of its probable causes and
629 possible agricultural consequences. *Agricultural and Forest Meteorology* 107, 255-278,
630 2001.

631 Stanhill, G., Achiman, O., Rosa, R. and Cohen, S. The cause of solar dimming and
632 brightening at the Earth's surface during the last half century: Evidence from
633 measurements of sunshine duration. *J. Geophys. Res. Atmos.* 119, 10902-10911.
634 doi:10.1002/2013JD021308, 2014.

635 Xavier, T. M. B. S., Silva Dias, M. A. F. and Xavier, A. F. S. Impact of ENSO episodes
636 on the autumn rainfall patterns near São Paulo, Brazil. *Int. J. Climatol.* 15. 571-584,
637 1995.

638 Wild, M., Gilgen, H., Roesch, A., Ohmura, A., Long, C. N., Dutton, E. G., Forgan, B.,
639 Kallis, A., Russak, V., and Tsvetkov, A. From dimming to brightening: decadal changes
640 in solar radiation at Earth's surface. *Science* 308, 847-850, 2005.

641 Wild, M., Ohmura, A., and Makowski, K. Impact of global dimming and brightening on
642 global warming. *Geophys. Res. Lett.* 34, L04702, doi: 10.1029/2006GL028031, 2007.

643 Wild, M. Global dimming and brightening: A review. *J. Geophys. Res.* 114(D00D16),
644 doi: 10.1029/2008JD011470, 2009.

645 Wild, M. Enlightening global dimming and brightening. *BAMS* 93, 27-37,
646 doi:10.1175/BAMS-D-11-00074.1, 2012.

- 647 Wild, M., Folini, D., Schär, C., Loeb, N., Dutton, E. G. and König-Langlo, G. The
648 global energy balance from a surface perspective. *Clim. Dyn.* 40, 3107-3134, doi:
649 10.1007/s00382-012-1569-8, 2013.
- 650 Wild, M. Towards global estimates of the surface energy budget. *Curr. Clim. Change*
651 *Rep.* 3, 87-97. doi: 10.1007/s40641-017-0058-x, 2017.
- 652 Yamasoe, M. A., N. M. E. do Rosário, and K. M. Barros. Downward solar global
653 irradiance at the surface in São Paulo city—The climatological effects of aerosol and
654 clouds, *J. Geophys. Res. Atmos.*, 122, 391–404, doi:10.1002/2016JD025585, 2017.
- 655 Yang, S., Wang, X. L. and Wild, M. Causes of Dimming and Brightening in China
656 Inferred from Homogenized Daily Clear-Sky and All-Sky in situ Surface Solar
657 Radiation Records (1958-2016). *Journal of Climate* 32, 5901-5913, doi: 10.1175/JCLI-
658 D-18-0666.1, 2019.
- 659 Zerefos, C.S., Eleftheratos, K., Meleti, C., Kazadzis, S., Romanou, A., Ichoku, C.,
660 Tselioudis, G. and Bais, A. Solar dimming and brightening over Thessaloniki, Greece,
661 and Beijing, China. *Tellus B*, 61: 657-665. doi:10.1111/j.1600-0889.2009.00425.x,
662 2009.
- 663 Zhang, S., W., J., Fan. W., Yang, Q. and Zhao, D. Review of aerosol optical depth
664 retrieval using visibility data. *Earth-Science Reviews* 200, 102986,
665 <https://doi.org/10.1016/j.earscirev.2019.102986>, 2020.